ELSEVIER

Tectonophysics 349 (2002) 297–308

TECTONOPHYSICS

www.elsevier.com/locate/tecto

He diffusion and (U–Th)/He thermochronometry of zircon: initial results from Fish Canyon Tuff and Gold Butte

Peter W. Reiners [a,*], Kenneth A. Farley [b,1], Hunter J. Hickes [a]

[a] *Department of Geology, Washington State University, Pullman, WA 99164-2812, USA*
[b] *Division of Geological and Planetary Sciences, MS 170-25, California Institute of Technology, Pasadena, CA 91125, USA*

Received 20 June 2000; accepted 27 July 2001

Abstract

To evaluate the potential of (U–Th)/He geochronometry and thermochronometry of zircon, we measured He diffusion characteristics in zircons from a range of quickly and slowly cooled samples, (U–Th)/He ages of zircons from the quickly cooled Fish Canyon Tuff, and age-paleodepth relationships for samples from 15 to 18 km thick crustal section of the Gold Butte block, Nevada. (U–Th)/He ages of zircons from the Fish Canyon Tuff are consistent with accepted ages for this tuff, indicating that the method can provide accurate ages for quickly cooled samples. Temperature-dependent He release from zircon is not consistent with thermally activated volume diffusion from a single domain. Instead, in most samples apparent He diffusivity decreases and activation energy (E_a) increases as cycled step-heating experiments proceed. This pattern may indicate a range of diffusion domains with distinct sizes and possibly other characteristics. Alternatively, it may be the result of ongoing annealing of radiation damage during the experiment. From these data, we tentatively suggest that the minimum E_a for He diffusion in zircon is about 44 kcal/mol, and the minimum closure temperature (T_c, for a cooling rate of 10 °C/myr) is about 190 °C. Age–paleodepth relationships from the Gold Butte block suggest that the base of the zircon He partial retention zone is at pre-exhumation depths of about 9.5–11 km. Together with constraints from other thermochronometers and a geothermal gradient derived from them in this location, the age–depth profile suggests a He T_c of about 200 °C for zircon, in reasonable agreement with our interpretation of the laboratory measurements. A major unresolved question is how and when radiation damage effects become significant for He loss from this mineral.

Keywords: Thermochronology; (U–Th)/He; Geochronology; Zircon; Helium

1. Introduction

Recent developments in (U–Th)/He dating have renewed interest in this very old method (Strutt, 1908), in particular for low temperature thermochronometry (Zeitler et al., 1987; Lippolt et al., 1994; Wolf et al., 1996, 1998; Farley et al., 1996; Warnock et al., 1997; Reiners and Farley, 1999; Farley, 2000). A wide range of studies has now confirmed the practical utility of He dating for constraining the timing and rates of exhumation and topographic development (Wolf et al., 1997; House et al., 1997, 1998; Spotila et al., 1998; Reiners et al., 2000). Other applications of He dating also hold potential, including elucidating the thermal

* Corresponding author. Present address: Department of Geology and Geophysics, Yale University, New Haven, CT 06511, USA. Tel.: +1-203-432-3761; fax: +1-203-432-3134.
E-mail address: peter.reiners@yale.edu (P.W. Reiners).
[1] Fax: +1-626-58-0935.

0040-1951/02/$ - see front matter
PII: S0040-1951(02)00058-6

histories of sedimentary basins (House et al., 1999), tephrachronology (Kohn et al., 1999, 2000), the timing of ore deposition and hydrothermal processes (McInnes et al., 1999), and cross-calibration with both fission-track and feldspar multidomain Ar dating.

To date, most work has focused on thermochronometry of apatite and titanite, but other U, Th-rich phases may provide additional tools for establishing the time-temperature paths of rocks. Zircon is a logical candidate to consider for He dating, but it has both potential advantages and disadvantages. U contents typically two to three orders of magnitude higher than in apatite or titanite yield large quantities of He in short time spans, making it potentially suitable for dating very young events (presuming potential complications from U-series diseqilibrium can be overcome). Additionally, owing to its relative stability at near-surface conditions and during transport, zircon is relatively abundant in some types of sedimentary rocks, and thus may be used to address problems such as sediment provenance and basin thermal histories that are not as easily accessible by apatite and titanite dating. Besides U- and Th-series disequilibrium in young samples, another potential complication associated with zircon is the effect of strong radiation damage (and slow damage annealing rate) on He diffusion characteristics.

Previous attempts to use the (U–Th)/He system to date zircon met with limited success. In general earlier studies found that He ages were younger than expected, assuming the ages should reflect time since formation of the crystals. Some of these studies noted an apparent correlation between radiation dosage and He "leakage" (Hurley, 1952), while other studies emphasized that radiation dosage was not the only control on He loss (Hurley et al., 1956; Damon and Kulp, 1957). The modern recognition that "young" (U–Th)/He ages in apatite and titanite reflect cooling ages rather than crystallization ages suggests the possibility that the early results on zircon have a similar explanation.

Here, we report age determinations on zircons from both quickly and slowly cooled rocks, as well as the results of preliminary He diffusion experiments on zircon, to evaluate the potential and possible complications of the method. Taken as a whole, our work suggests that zircon closes to He loss at about 200 °C, similar to titanite. This constraint is derived primarily from observations of age–paleodepth relationships in the Gold Butte block, however, and is only qualitatively consistent with the step heating experiments, which indicate that He diffusivity from zircon is more complex than in apatite or titanite.

2. Samples and methods

We performed step-heating diffusion experiments on zircons from the quickly cooled Fish Canyon Tuff, Colorado, and slowly cooled specimens from the Chain of Ponds pluton, Maine, and the Gold Butte block, south Virgin Mountains, Neveda. The Chain of Ponds pluton has an intrusive age of about 375 Ma (Heizler et al., 1988). For the Fish Canyon Tuff, apatite and zircon fission track dates yield 26.8 ± 4.2 and 27.9 ± 2.2 Ma, respectively (Carpéna and Mailhé, 1987), and biotite and feldspar $^{40}Ar/^{39}Ar$ dates yield 27.8 ± 0.2 (Hurford and Hammerschmidt, 1985) and 28.03 ± 0.18 Ma (Renne et al., 1994), respectively. Reiners and Farley obtained an average age of 30.1 ± 1.0 Ma for (U–Th)/He dates on Fish Canyon Tuff titanite. House et al. (2000) revised that number, through laser-extraction methods, to 27.9 ± 1.1 Ma.

The Gold Butte block is a largely intact 15–18 km thick section of 1.4–1.7 Ga crystalline rock that was rapidly exhumed by normal faulting at 15–16 Ma, providing excellent exposure of a tilted shallow-to-mid crustal section (Volborth, 1962; Wasserburg and Lanphere, 1965; Silver et al., 1977; Wernicke and Axen, 1988; Fitzgerald et al., 1991; Fryxell et al., 1992; Reiners et al., 2000; Brady et al., 2000). The Gold Butte zircons used for diffusion experiments comprise two samples from the same pluton but different pre-exhumation paleodepths and therefore long-term thermal histories. 98PRGB18 resided at approximately 90 °C prior to exhumation at 16 Ma, while 98PRGB4 resided at approximately 310 °C (Reiners et al., 2000).

Nearly all the zircon crystals we examined from these rocks contained inclusions of other minerals. While we avoided picking crystals with the largest and most abundant inclusions, most of the aliquots used for diffusion and dating purposes inevitably did contain grains with some $\sim 1–10$ μm inclusions (Fig. 1). Back-scattered electron images of representative zircons reveal that mineral inclusions in the

Fig. 1. Backscattered electron images taken on the WSU electron microprobe of zircons from Fish Canyon Tuff (FCT) and the Gold Butte granite at pre-exhumation paleodepths of 15 (GB4) and 4 km (GB18). The two large inclusions in the FCT zircon are alkali-feldspar with minor quartz. Subtle compositional zonation is indicated by the weak concentric shading zonation in FCT. Inclusions in the GB4 zircon are alkali-feldspar ± quartz, except for the largest inclusion in the lower-right corner of the crystal, which is biotite. Inclusions in GB18 zircons are also dominantly alkali-feldspar ± quartz; small inclusion labelled "py" in center grain is iron-sulfide. Weak concentric compositional zonation is apparent in these (but not all) GB18 zircons.

Fish Canyon Tuff crystals were dominantly alkali feldspar or quartz; no other high-U, Th phases were observed in the 10 crystals examined with an electron microprobe. Alkali-feldspar and quartz were also the most abundant inclusion types in Gold Butte zircons, but these also contained less abundant FeS (pyrite?), apatite, and biotite inclusions. Fish Canyon Tuff and Gold Butte zircons showed little discernable compositional zonation in back-scattered electron imaging, although subtle concentric zonation was present in a few grains (Fig. 1).

Age determinations were also performed on Fish Canyon Tuff and Gold Butte zircons, the latter from a range of pre-exhumation paleodepths, from 4 to 16 km. Euhedral zircon crystals (~ 60–120 μm width and ~ 150–300 μm length) were picked from aliquots prepared by standard mineral separation techniques (crushing, sieving, magnetic and density separations).

He diffusion experiments were performed at Caltech and used approximately 10–15 crystals that were rinsed in cold 10% HNO_3 to remove potential adhering phosphates. One aliquot of Fish Canyon Tuff zircons was crushed and sieved to a size range of 44–74 μm to examine the effect of grain size on diffusivity. The second aliquot consisted of grains with typical radii and lengths of 60 and 150 μm, respectively. The experimental apparatus and procedures followed those described by Farley et al. (1999), involving cycled step-heating of the crystals in a high vacuum chamber by a lamp projected through a sapphire window. Temperatures ranged from 280 to 600 °C, with durations ranging from 30 to 420 min. Estimated accuracy of the temperature measurements is ± 3 °C based on stated thermocouple characteristics; within-run temperature stability during each step is better than ± 1 °C. All experiments were cycled (i.e., included step sequences of both increasing and decreasing temperature). Most experiments had step sequences that first increased and then decreased in temperature. Run-up and cool-down times between steps (durations required for sample to reach temperature setpoint or cool to temperature significantly below that of the experiment) were less than 1–3 minutes and are insignificant for diffusivity measurements compared with the isothermal holding times. ^{4}He released from the sample in each step was measured by a quadrupole mass spectrometer using ^{3}He isotope dilution. He blanks were determined throughout the temperature range of our experiments and showed no time or temperature dependence; cold blanks were checked prior to each run and a typical blank of 0.02 ncc (STP) of ^{4}He (< 0.05% of typical ^{4}He released at 500 °C) was subtracted from each step. Average 1σ reproducibility of ^{4}He standards comparable in size to the sample extractions is better than 1%. Diffusivity calculations require knowledge of cumulative fraction of He released in each step, so the final step of each experiment was total fusion of the grains. Because our

diffusion apparatus cannot achieve temperatures greater than about 800 °C, we used a resistively heated furnace and measured the residual He content on a MAP 215-50 mass spectrometer by peak height comparison to standards (for details, see Wolf et al., 1996). For consistency with previous work, our calculations

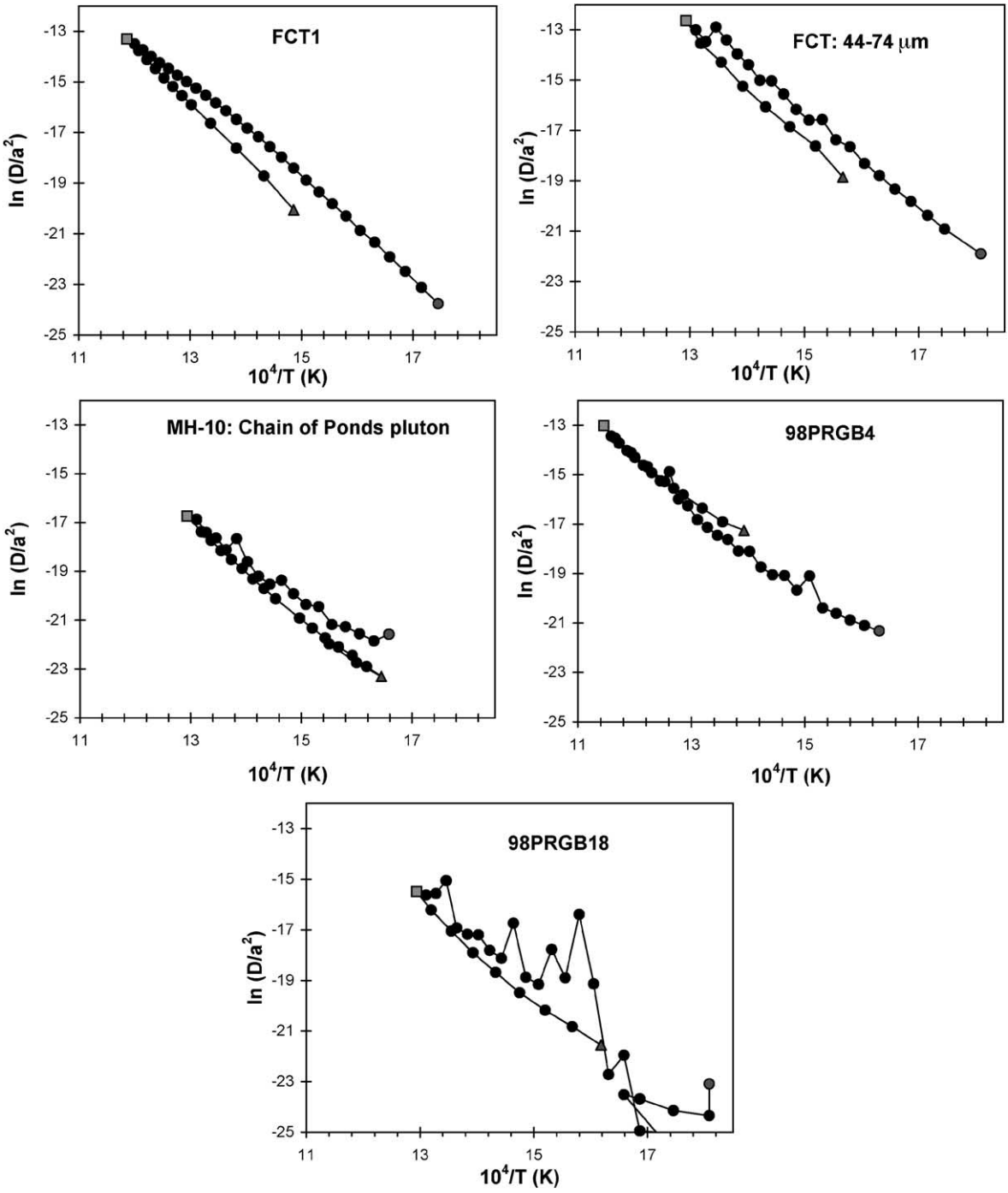

Table 1
Zircon diffusion data and closure temperatures inferred from portions of the diffusion experiments

Sample	E_a, up T steps (kcal/mol)	D_0/a^2 (s^{-1})	E_a, down T steps (kcal/mol)	D_0/a^2 (s^{-1})	T_c for down T steps (°C)
FCT1	37.1	9491	44.1	4.367×10^5	189
FCT44-74	37.3	1.451×10^5	43.2	3.997×10^6	160
MH-10	29.4	9.563	36.6	870.4	166
98PRGB4	29.2	10.89	34.6	779.9	144
98PRGB18	?	?	36.9	3472	156

of diffusivity (D/a^2, Fechtig and Kalbitzer, 1966) and closure temperature (T_c, Dodson, 1973) assume spherical geometry of diffusion domains.

Age determinations were performed on aliquots of one to six individual euhedral zircon crystals. Half of the ages were determined at Caltech, and half at Washington State University. In both laboratories, the aliquots of crystals were placed in 1-cm stainless steel capsules, sequentially dropped into a resistively heated UHV furnace, and heated to about 1200 °C for 30 min. Evolved gases were processed through a sequence of getters and a charcoal cryotrap cycling between 16 and 37 K. In the Caltech sample group, ^{4}He contents for about half the samples were measured by standard peak height comparison on a MAP 215-50 mass spectrometer, and the others by isotope dilution (^{3}He) on a quadrupole mass spectrometer. Both methods have an estimated precision of about $\pm 1\%$ (1σ). Pre-run furnace blanks were less than 0.02 ncc (STP) ^{4}He. Subsequent heating of each sample at 1200 °C for 20 min (re-extracts) typically yielded 0.1–0.5% of the total extracted He, indicating near-quantitative He extraction. Grains were then retrieved from the capsules and placed in teflon vials, spiked with ^{230}Th and ^{235}U, and dissolved with HF-HNO_3 in a teflon lined steel bomb held at 235 °C for 3 days. Following bombing and evaporation of the HF, the samples were rehydrated with 5% HNO_3. The resulting solution was analyzed for ^{238}U/^{235}U and ^{232}Th/^{230}Th ratios using a self-aspirating micro-concentric nebulizer and standard torch on a Finnigan Element sector ICP-MS. Estimated uncertainty on the U and Th measurements is $<1\%$ (1σ). Sample procedures and analytical details for the WSU samples are the same as for the Caltech ones, except: (1) pre-run blanks were <0.04 ncc STP ^{4}He, (2) zircons were spiked with ^{229}Th and ^{233}U, (3) following HF-HNO_3 bombing, samples were rebombed at 200 °C for 24 h in concentrated HCl, and (4) ^{232}Th/^{229}Th and ^{238}U/^{233}U were measured using a teflon micro-concentric nebulizer and standard torch on a HP-4500 Plus quadropole ICP-MS. Raw He ages of all samples were corrected for the effects of alpha ejection using the approach of Farley et al. (1996), modified for the tetragonal prism morphology and density of zircon. Wolf et al. (1996) have shown that no measurable U or Th loss occurs during heating of apatite up to 1100 °C. While we have not conducted similar experiments with zircon, good agreement between (U–Th)/He ages and ages determined by other methods on Fish Canyon Tuff zircon suggest the same results.

3. Results

3.1. He diffusion

Fig. 2 shows Arrhenius plots for the step-heating diffusion experiments. To a greater or lesser degree all samples yield a negative correlation between He

Fig. 2. Arrhenius plots for cycled step-heating He diffusion experiments for zircons from Fish Canyon Tuff (FCT1), crushed and sieved Fish Canyon Tuff (FCT: 44–74 μm), the Chain of Ponds pluton (MH-10), and Gold Butte (98PRGB4 = pre-exhumation paleodepth of 14.8 km; 98PRGB18 = pre-exhumation paleodepth of 3.9 km). All experiments comprise steps that began at low temperature (grey circle), increased to high temperature (grey square), and then decreased again to low temperature (grey triangle). Most samples show initial up-temperature steps with relatively high and (except for the case of FCT1) erratic diffusivity variations, followed by down-temperature steps with lower and less erratic diffusivity. 98PRGB4 shows the opposite however, with relatively low diffusivity in the initial up-temperature steps and higher diffusivity in later, down-temperature steps. See text for discussion and Table 1 for inferred E_a, D_0/a^2, and T_c for up- and down-temperature portions of the experiments.

diffusivity and reciprocal temperature, as expected for a thermally activated diffusion process. However, several aspects of the data are not consistent with this simple interpretation.

He diffusivity in zircon is the best behaved in the FCT samples. In both aliquots, diffusivities plot on well-defined, slightly curved arrays. However, diffusivities at a given temperature are higher in the initial up-temperature sequence than in the later down-temperature sequence. In addition, the slopes of the Arrhenius trends are distinct, such that activation energies (E_a), determined from the down-temperature trends are higher (43–44 kcal/mol) than those for the up-temperature trends (37 kcal/mol) Table 1. This discrepancy between up-temperature and down-temperature steps is similar in magnitude in the two grain-size fractions. However, the intercepts (D_0/a^2) of the trends for the fine-grained zircons are always higher than those of the whole crystals. The Chain of Ponds sample (MH-10) yields a similar overall pattern and range of activation energies as the FCT zircons, but with occasional data points lying above the well-defined array.

98PRGB4, the Gold Butte sample from 15 km pre-exhumation paleodepth, also yields a slightly curved array, but with lower diffusivity in the initial low-temperature steps, and slightly higher slope in the trend of the down-temperature steps (E_a of up-T steps = 29 kcal/mol, E_a of down-T steps = 35 kcal/mol). Again occasional data points lie above the main trend. Finally, in contrast to the other samples, 98PRGB18 yields generally high and "spiky" diffusivity in the up-temperature steps, with no obvious trend with temperature. However, following heating to 500 °C, the down-temperature steps lie on a more linear trend with inverse temperature, yielding E_a of 37 kcal/mol, comparable to the other samples.

3.2. Age determinations

(U–Th)/He ages of eight FCT zircons range from 26.4 to 29.2 Ma (Table 2), with a mean of 27.3 ± 2.1

Table 2
(U–Th)/He data for Fish Canyon Tuff and Gold Butte block zircons

Sample	Paleodepth (km)	U (ppm)	Th (ppm)	He (ncc/mg)	Mass (μg)	No. of crystals	m.w.a. radius	m.w.a. length	F_T	Raw age	Corr. age	+/− (2σ)
Fish Canyon Tuff												
FCTZrc-CIT	N/A	463	240	1359	10.8	2	46	139	0.76	21.3	28.1	2.2
FCTZrd-CIT	N/A	251	96	701	26.8	3	48	218	0.79	20.9	26.4	2.1
FCTZr1-WSU	N/A	372	148	1092	29.6	2	46	262	0.79	22.2	28.1	2.2
FCTZr2-WSU	N/A	349	173	1040	42.7	3	58	364	0.83	22.1	26.6	2.1
FCTZr3-WSU	N/A	196	121	586	21.9	2	54	246	0.81	21.6	26.6	2.1
FCTFL-WSU	N/A	219	112	629	22.1	2	35	230	0.80	21.2	26.5	2.1
FCTFL2-WSU	N/A	288	212	911	33.8	2	52	270	0.83	22.3	26.8	2.1
FCTZr5-WSU	N/A	362	199	1024	6.87	2	35	170	0.71	20.7	29.2	2.3
Mean											27.3	2.1
Gold Butte block												
98PRGB2-CIT	16.3	150	26.6	281	46.4	5	46	258	0.78	14.9	19.1	1.5
98PRGB4B-CIT	14.9	118	53.2	354	164	6	66	418	0.85	22.2	25.9	2.1
98PRGB4-WSU	14.9	75.0	50.4	194	18.9	3	39	230	0.75	18.5	24.7	2.0
98PRGB6-CIT	13.0	67.8	22.0	122	85.9	5	59	290	0.83	13.9	16.7	1.3
98PRGB9-CIT	11.2	96.7	39.3	267	131	6	58	413	0.83	20.7	24.5	2.0
98PRGB9-WSU	11.2	174	24.2	486	10.2	2	34	234	0.72	19.8	27.5	2.2
98PRGB12A-CIT	9.3	65.4	20.5	242	92.2	5	53	364	0.82	28.5	34.8	2.8
98PRGB12B-CIT	9.3	86.9	33.0	415	142	4	68	470	0.86	35.9	41.4	3.3
98PRGB16-CIT	7.1	144	44.4	1582	71.8	4	56	341	0.82	84.1	102	8.2
98PRGB16-WSU1	7.1	89.0	76.0	1057	5.76	1	32	63	0.71	81.3	115	9.2
98PRGB16-WSU2	7.1	133	66	1715	4.99	1	96	296	0.88	95.0	107	8.6
98PRGB18-CIT	3.9	300	118	5690	94.7	3	68	413	0.85	141	163	13

m.w.a. is mass weighted average. F_T is alpha-ejection correction parameter of Farley et al. (1996).

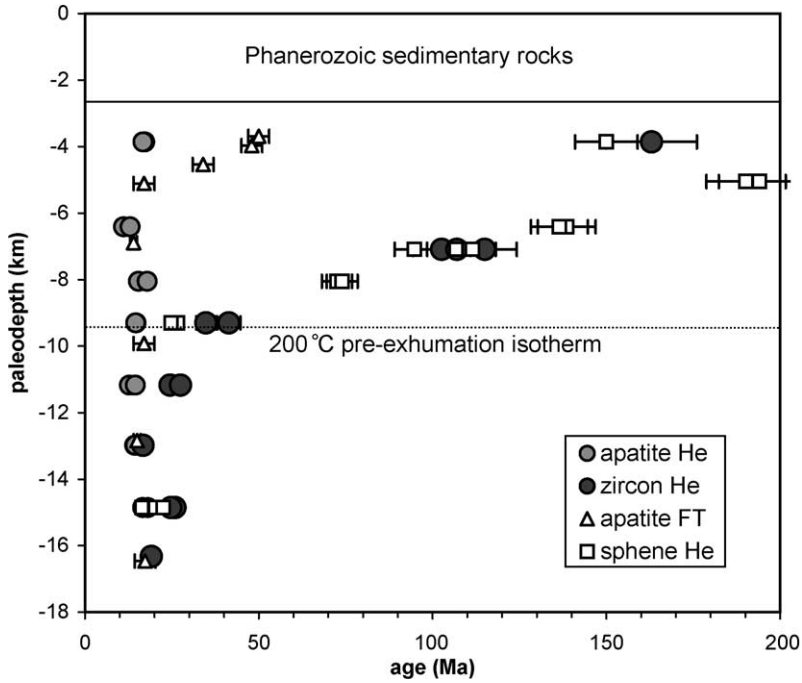

Fig. 3. Fission track (from Fitzgerald et al., 1991) and (U–Th)/He thermochronometry of Gold Butte block samples (apatite and titanite He ages from Reiners et al., 2000). Zircon He ages are relatively low (17–26 Ma) at paleodepths below about 9.5–11 km, then increase rapidly at shallower paleodepths, suggesting the base of the zircon He partial retention zone (PRZ) at 9.5–11 km. Based on other results from other thermochronometers, these paleodepths would correspond to a pre-exhumation isotherm of about 200–230 °C, suggesting a closure temperature (T_c) of about this temperature. Error bars on zircon He ages are ± 8% (2σ).

(8%, 2σ). Based on the reproducibility of the FCT zircons here, as well as our experience with apatite and titanite He dating, a reasonable estimate for the true uncertainty on zircon He ages is probably about ± 8% (2σ). A significantly larger number of zircon He dates must be made to obtain a more precise estimate of the error.

At least part of the 8% reproducibility (considerably higher than the ~ 2% (2σ) analytical uncertainty) probably has an origin in U and Th zonation within the crystals. Farley et al. (1996) examined the effects of zonation in apatite, concluding that extreme zonation (50-fold exponential increase from core to rim), could lead to alpha-ejection corrections in error by about 12%. Similar results would apply to zircon.

Gold Butte zircons range in age from 16.7 ± 1.7 to 163 ± 16 Ma (2σ), with younger ages in the structurally lower parts of the block (Fig. 3). There is a prominent break in slope between samples from 9 and 11 km. Assuming the pre-exhumation geothermal gradient of 20 °C/km inferred from other studies of Gold Butte (Fitzgerald et al., 1991; Reiners et al., 2000) and a 10 °C ambient surface temperature, the pre-exhumation temperature at 10 km depth would have been about 210 °C.

4. Discussion

4.1. He diffusion in zircon

In contrast to previous results for apatite and titanite (Wolf et al., 1996; Farley, 2000; Reiners and Farley, 1999), the Arrhenius plots for He diffusion in zircon from all of the samples shown here are not easily reconciled with simple volume diffusion from a single domain. Three features of the experiments are difficult to explain: (1) apparently distinct intercepts for trends of up-T and down-T steps for all of the runs, (2) increasing slopes of diffusivity vs. inverse T as the

experiment progressed (especially in the cases of FCT1 and MH-10), and (3) the highly erratic He diffusivity in the initial up-T steps most prominent in sample 98PRGB18.

The slightly higher D_0/a^2 for the crushed sample of FCT zircon, relative to the whole FCT crystals, is consistent with a grain size control on diffusivity. This suggests that, like apatite and titanite, the size of the diffusion domain a may be that of the grain itself. More experiments are necessary to confirm this suggestion however, partly because the average radius of the whole FCT crystals (60 μm) is similar to and within the range of the mesh sizes of the crushed and sieved FCT fraction (44–74 μm).

The changing slopes and apparently decreasing diffusivity with time in each experiment has several possible explanations. One is that He is heterogeneously distributed within the crystals in a way that decreases the apparent diffusivity during each experiment. We feel that this is unlikely however, given the two most likely origins of He zonation. One possible cause is loss from the rim of the crystals by either alpha-ejection or diffusion. This effect, which was observed in the case of whole titanite grains (Reiners and Farley, 1999), would actually have the opposite effect—that of increasing apparent diffusivity during the experiment. Another potential cause of He zonation is U and Th zonation in the crystal. To explain the consistently decreasing apparent diffusivity in all the samples however, U and Th would have to be consistently enriched towards the crystal rims in all samples analyzed. Backscattered electron images of the FCT and GB zircons also do not provide any evidence for strong compositional zonation, though this does not necessary rule out U and Th zonation.

Another possibility is that radiation damage has affected He diffusivity and this damage is progressively annealed, reducing diffusivity and increasing activation energy, during the experiment. Annealing studies of zircon show that on 1-h timescales, fission tracks begin to shorten at about 450–500 °C—within the range of temperatures achieved in our experiments (Tagami et al., 1990; Yamada et al., 1995). Radiation damage leading to metamictization, however, is thought to be caused not by fission, but by alpha damage, for which the temperature influence on annealing rates is not well known. Tagami et al. (1990) inferred some alpha damage annealing on 1-h timescales at 450–500 °C, whereas Yamada et al. (1995) reported it at 550–600 °C. In contrast, Murakami et al. (1991) could not confirm any alpha damage annealing at temperatures of 750 °C, and suggested that much higher temperatures (>1000 °C) are required. If the lower range of estimates is correct, then either fission track or some alpha damage annealing could have occurred during the higher temperature portions of our experiments. Presuming that radiation damage causes increased diffusivity and decreased E_a, and thermal annealing reduces these effects, our diffusion results are qualitatively consistent with the effects of annealing during each experiment. A similar origin for observed changes in He diffusivity in relatively high temperature portions of experiments has previously been proposed in the case of Durango apatite (Farley, 2000).

Another possibly related explanation for the complex He diffusion behavior is that multiple domains of different size or diffusion characteristics are present within each sample (e.g., Lovera et al., 1991). This could not be caused solely by variations in crystal size within each sample, as crystal sizes within each aliquot did not vary by more than about 15%. Thus, the hypothetical distinct domains would have to be intracrystalline. Our current results do not allow us to adequately evaluate this possibility. However, simple multi-domain forward modeling of synthetic step-heating diffusion data reveals that if the domains were different in size alone, a sizeable fraction of each crystal (~ 30%) would have to contain domains with a range of sizes (approximately 10–30 μm) in addition to a domain corresponding to the average crystal radius (typically 60–120 μm).

One possible explanation for the source of these hypothetical intracrystalline domains is a range of length scales associated with the micro-fracturing that has been shown to accompany differential expansion of zircon crystals caused by inhomogeneously distributed radiation damage. Chakoumakos et al. (1987) and other authors (e.g., Peterman et al., 1986) have documented abundant microfractures in zircons radiating away from high U and Th zones that are, at least in some cases, metamict. The spacing between these fractures, which is typically some fraction of the thickness of the high U and Th zones (tens of μm), could yield a range of He diffusion domain sizes that produces the characteristics observed in Fig. 2. It is

also possible that domains could differ not only in size but also in E_a and/or D_0. Some fractures were observed in backscattered electron images of these zircons, which may be at least partly related to these results.

In any case, the gradually decreasing slopes and diffusivity observed as most of the experiments progressed could indicate either exhaustion of He within volumes between microfractures, within zones of intense radiation damage, or possibly a progressive annealing of the crystal structure within damage zones. The decrease in erratic diffusivity in both MH-10 and 98PRGB18 samples following heating to the highest temperature of the experiments (500–600 °C) are qualitatively consistent with all of these interpretations.

The wide range in apparent E_a, and D_0/a^2, and thus computed T_c, both within and among the experiments shown here, preclude confident assignment of a closure temperature to the (U–Th)/He system in zircon. If the gradual decrease in diffusivity and increase in E_a observed with time in most of the experiments indicate progressive annealing of radiation damage, then the most accurate estimates of E_a and T_c for "fresh" zircon are probably higher than any derived from the diffusion experiments. This is at least partly because the slopes of the Arrhenius trends are affected by all previous steps, and significantly higher apparent diffusivity in the early steps causes artificially shallow slopes of overall trends even if small or less-retentive domains are exhausted of He. Thus we suggest that the highest E_a obtained from these experiments (44.1 kcal/mol on the down-T steps of FCT1) is probably a minimum E_a for He diffusion in zircon. The computed T_c (for $dT/dt = 10$ °C/myr) for this portion of this experiment is also the highest, 190 °C; this may be a minimum T_c for the zircon (U–Th)/He system.

4.2. Age determinations

Ages of FCT zircons are consistent with the accepted age of this tuff (Hurford and Hammerschmidt, 1985; Carpéna and Mailhé, 1987), indicating that the (U–Th)/He system provides reliable ages on quickly cooled samples.

The overall distribution of zircon (U–Th)/He ages from the Gold Butte block (Fig. 3) is consistent with age–paleodepth relationships from other techniques including apatite fission track dating (Fitzgerald et al., 1991), and (U–Th)/He dating of apatite and titanite (Reiners et al., 2000). These earlier studies revealed Miocene cooling ages (~ 15–16 Ma) at the bottom of the block, with older ages (reflecting fossil fission track partial annealing or He partial retention zones (HePRZ; Wolf et al., 1998) at shallower paleodepths. Zircon ages of the structurally lowest samples however, range in age from 17 to 26 Ma—older than the 15–16 Ma ages from other systems at the same depths. We do not have an explanation for this, as other systems show no indication of earlier cooling. It is noteworthy, however, that given typical U and Th contents of the zircons in the lower part of the section, an additional fraction of only 0.3–0.5% of the ^{4}He produced within the zircon would have to be retained over the 1.45 Ga age of the crystals in order to shift the (U–Th)/He ages from 16 to 25 Ma today. It is conceivable, though difficult to test at this point, that some part of these zircons could have trapped very small excess fractions of the total of He produced in the grains. One potential mechanism for such He retentivity in excess of that predicted by volume diffusion is trapping of He in radiation damage zones.

Despite these complications in the lower part of the Gold Butte section, the rapid increase in age with shallower structural depth is consistent with the base of a fossil partial retention zone at about 9.5–11 km paleodepth, similar to that observed for the titanite (U–Th)/He system (Reiners et al., 2000). In the case of titanite, diffusion experiments clearly indicate a T_c of about 190–210 °C, which agrees with other constraints indicating a pre-exhumation geothermal gradient of about 20 °C/km. Thus the break in slope at about 9.5–11 km paleodepth for zircon (U–Th)/He ages provides an independent estimate of about 200–230 °C for the closure temperature of this system. This value is consistent with the minimum T_c of 190 °C inferred from the diffusion experiments above.

5. Potential effects of radiation damage and "effective T_c"

The relative (U–Th)/He ages, thermal histories, and diffusion characteristics for the two Gold Butte samples from the same 1.45-Ga pluton may be important for understanding the origin of the unusual and com-

plex behavior of He diffusion in zircon. Diffusion results for sample 98PRGB18, the Gold Butte sample from the shallowest paleodepth and lowest pre-exhumation temperature are the most erratic of all samples in the initial up-temperature steps. Following steps at high temperature (500 °C) however, the diffusivity appears to be well-correlated with inverse temperature, and similar to that observed in sample 98PRGB4, which has a high pre-exhumation temperature of about 310 °C. If some type of radiation damage exerts a control over diffusivity, and its effects are annealed or otherwise reduced by heating at high temperature (e.g., 500 °C on a laboratory timescale and 300 °C on a geologic timescale), it may explain both the apparent decrease in erratic diffusivity following heating to high temperatures in diffusion experiments, as well as the relatively "normal" diffusion characteristics exhibited by the Gold Butte sample from greater paleodepths and higher pre-exhumation temperature. Annealing of zircon fission tracks occurs over geologic timescales at temperatures of about 200–250 °C (Fleischer et al., 1965; Murakami et al., 1991; Yamada et al., 1995), intermediate between the long-term holding temperatures of the two Gold Butte samples. Clearly more work is needed to resolve the relative effects of radiation dosage and thermal history on He diffusion, but this may indicate that samples with high alpha dosages and long-term histories at low temperatures have different He retentivity and release characteristics (which produce relatively high and erratic apparent diffusivity in Arrhenius plots) than "normal, fresh" zircon.

If the above analysis is correct, it raises the complicated question of how He diffusivity might vary over the time-history of a zircon crystal, and what the appropriate, integrated diffusion characteristics and T_c would be for any given (U–Th)/He dated sample. Our data suggest that minimally radiation-damaged crystals have higher closure temperatures (>190 °C) than more damaged crystals (with at least some regions with T_c perhaps as low as 140–160 °C. Surprisingly, the inferred position of the zircon He partial retention zone from the Gold Butte section is most consistent with a T_c of no lower than about 200°C, not the lower T_c that may be inferred for these radiation damaged crystals. Thus, on the basis of the Gold Butte data, we tentatively suggest a T_c in the range of 200–230 °C for He in zircon. But before this value can be invoked with any confidence a more quantitative assessment of radiation damage effects and the origin of the peculiar He release kinetics (Fig. 2) are required.

6. Conclusions

(U–Th)/He ages of zircons from the Fish Canyon Tuff are consistent with the accepted age of this tuff, demonstrating that absolute dating of zircon (at least with this degree of radiation damage) is feasible. However, He diffusion in zircon is more complex than in apatite or titanite, and is not consistent with thermally activated volume diffusion from a single domain. Apparent diffusivities decrease and activation energies increase during cycled step-heating experiments. Average E_a of down-temperature portions of step-heating cycles range from 35 to 44 kcal/mol, yielding closure temperatures for the (U–Th)/He system (assuming a cooling rate of 10 °C/Ma) of 144–190 °C. Although not conclusive, these characteristics are consistent with diffusion from a mixture of intracrystalline domains with distinct diffusion characteristics. If diffusion domain size is the only control, then crystals contain a range of domain sizes including a large fraction (~ 30%) with effective radii ~ 10–30 μm. (U–Th)/He ages of zircons from a range of pre-exhumation paleodepths and temperatures in the Gold Butte block yield a range of ages that suggest the base of a fossil He partial retention zone at about 9.5–11 km paleodepth, or 200–230 °C pre-exhumation temperature. These data suggest that the effective closure temperature for the (U–Th)/He zircon dating is in the range 200–230 °C. The probable role of radiation damage on these parameters warrants further investigation.

Acknowledgements

Thanks to Barry Kohn for the FCT samples, Matt Heizler for the Chain of Ponds sample, Mark Garcia for mineral separations, Lindsey Hedges for help with zircon dissolutions at Caltech, Charles Knaack for technical and analytical help at WSU, Scotty Cornelius for microprobe help, and Rob Brady for help in the field at and with geologic interpretation of

Gold Butte. We appreciate constructive and thought-provoking reviews from Fin Stuart and Mark Harrison. This work was supported in part by NSF EAR 0073576 to PWR and NSF grants to KAF.

References

Brady, R., Wernicke, B., Fryxell, J., 2000. Evolution of a large-offset continental normal fault system, South Virgin Mountains, Nevada. Geol. Soc. Am. Bull. 112, 1375–1397.

Carpéna, J., Mailhé, D., 1987. Fission-track dating calibration of the Fish Canyon Tuff standard in French reactors. Chem. Geol. 66, 53–59.

Chakoumakos, B.C., Murakami, T., Lumpkin, G.R., Ewing, R.C., 1987. Alpha-decay-induced fracturing in zircon: the transition from the crystalline to the metamict state. Science 236, 1556–1559.

Damon, P.E., Kulp, J.L., 1957. Determination of radiogenic helium in zircon by stable isotope dilution technique. Trans. Am. Geophys. Union 38, 945–953.

Dodson, M.H., 1973. Closure temperature in cooling geochronological and petrological systems. Contrib. Mineral. Petrol. 40, 259–274.

Farley, K.A., 2000. Helium diffusion from apatite: general behavior as illustrated by Durango fluorapatite. J. Geophys. Res. 105, 2903–2914.

Farley, K.A., Wolf, R.A., Silver, L.T., 1996. The effects of long alpha-stopping distances on (U–Th)/He ages. Geochim. Cosmochim. Acta 60, 4223–4229.

Farley, K.A., Reiners, P.W., Nenow, V., 1999. An apparatus for measurement of noble gas diffusivities from minerals in vacuum. Anal. Chem. 71, 2059–2061.

Fechtig, H., Kalbitzer, S., 1966. The diffusion of argon in potassium-bearing solids. In: Schaeffer, O.A., Zahringer, J. (Eds.), Potassium–Argon Dating. Springer, Berlin, pp. 68–106.

Fitzgerald, P.G., Fryxell, J.E., Wernicke, B.P., 1991. Miocene crustal extension and uplift in southeastern Nevada: constraints from fission track analysis. Geology 10, 1013–1016.

Fleischer, R.L., Price, P.B., Walker, R.M., 1965. Effects of temperature, pressure and ionization on the formation and stability of fission tracks in minerals and glasses. J. Geophys. Res. 70, 1497–1502.

Fryxell, J.E., Salton, G.G., Selverstone, J., Wernicke, B., 1992. Gold Butte crustal section, South Virgin Mountains, Nevada. Tectonics 11, 1099–1120.

Heizler, M.T., Lux, D.R., Decker, E.R., 1988. The age and cooling history of the Chain of Ponds and Big Island Pond Plutons and The Spider Lake Granite, west-central Maine and Quebec. Am. J. Sci. 288, 925–952.

House, M.A., Wernicke, B.P., Farley, K.A., Dumitru, T.A., 1997. Cenozoic thermal evolution of the central Sierra Nevada, California, from (U–Th)/He thermochronometry. Earth Planet. Sci. Lett. 151, 167–179.

House, M.A., Wernicke, B.P., Farley, K.A., 1998. Dating topography of the Sierra Nevada, California, using apatite (U–Th)/He ages. Nature 396, 66–69.

House, M.A., Farley, K.A., Kohn, B.P., 1999. An empirical test of helium diffusion in apatite: borehole data from the Otway basin, Australia. Earth Planet. Sci. Lett. 170, 463–474.

House, M.A., Farley, K.A., Stockli, D., 2000. Helium chronometry of apatite and titanite using Nd-YAG laser heating. Earth Planet. Sci. Lett. 183, 365–368.

Hurford, A.J., Hammerschmidt, K., 1985. $^{40}Ar/^{39}Ar$ and K/Ar dating of the Bishop and Fish Canyon Tuffs: calibration ages for fission-track dating standards. Chem. Geol. 58, 23–32.

Hurley, P.M., 1952. Alpha ionization damage as a cause of low helium ratios. Trans. Am. Geophys. Union 33, 174–183.

Hurley, P.M., Larsen Jr., E.S., Gottfried, D., 1956. Comparison of radiogenic helium and lead in zircon. Geochim. Cosmochim. Acta 9, 98–102.

Kohn, B.P., Farley, K.A., Pillans, B., 1999. (U–Th)/He dating of zircon and apatite from the Pleistocene Rangitawa tephra, North Island, New Zealand. Trans. Am. Geophys. Union 80, 1169.

Kohn, B.P., Farley, K.A., Pillans, B., 2000. (U–Th)/He and fission track dating of the Pleistocene Rangitawa tephra, North Island, New Zealand: a comparative study. Geological Society of Australia Abstract Series No. 58, 207.

Lippolt, H.J., Leitz, M., Wernicke, R.S., Hagedorn, B., 1994. (Uranium + thorium)/helium dating of apatite: experience with samples from different geochemical environments. Chem. Geol. 112, 179–191.

Lovera, O.M., Richter, F.M., Harrison, T.M., 1991. Diffusion domains determined by ^{39}Ar released during step heating. J. Geophys. Res. 96, 2057–2069.

McInnes, B.I.A., Farley, K.A., Sillitoe, R.H., Kohn, B.P., 1999. Application of apatite (U–Th)/He thermochronometry to the determination of the sense and amount of vertical fault displacement at the Chuquicamata porphyry copper deposit, Chile. Econ. Geol. 94, 937–948.

Murakami, T., Chakoumakos, B.C., Ewing, R.C., Lumpkin, G.R., Weber, W.J., 1991. Alpha-decay event damage in zircon. Am. Mineral. 76, 1510–1532.

Peterman, Z.E., Zartman, R.E., Sims, P.K., 1986. A protracted Archean history in the Watersmeet gneiss dome, northern Michigan. U.S. Geol. Surv. Bull. 1622, 51–64.

Reiners, P.W., Farley, K.A., 1999. He diffusion and (U–Th)/He thermochronometry of titanite. Geochim. Cosmochim. Acta 63, 3845–3859.

Reiners, P.W., Brady, R., Farley, K.A., Fryxell, J.E., Wernicke, B.P., Lux, D., 2000. Helium and argon thermochronometry of the Gold Butte block, South Virgin Mountains, Nevada. Earth Planet. Sci. Lett. 178, 315–326.

Renne, P.R., Deino, A.L., Walter, R.C., Turrin, B.D., Swisher III, C.C., Becker, T.A., Curtis, G.H., Sharp, W.D., Jaouni, A.-R., 1994. Intercalibration of astronomical and radioisotopic time. Geology 22, 783–786.

Silver, L.T., Bickford, M.E., Van Schmus, W.R., Anderson, J.L., Anderson, T.H., Medaris Jr., L.G. 1977. The 1.4–1.5 b.y. transcontinental anorogenic plutonic perforation of North America. Geol. Soc. Am. Abs. Prog. 9, 1176–1177.

Spotila, J.A., Farley, K.A., Sieh, K., 1998. Uplift and erosion of the

San Bernardino Mountains associated with transpression along the San Andreas fault, California, as constrained by radiogenic helium thermochronometry. Tectonics 17, 360–378.

Strutt, R.J., 1908. On the accumulation of helium in geological time. Proc. R. Soc., Ser. A 81, 272–277.

Tagami, T., Ito, H., Nishimura, S., 1990. Thermal annealing characteristics of spontaneous fission tracks in zircon. Chem. Geol. 80, 159–169.

Volborth, A., 1962. Rapakivi-type granites in the Precambrian complex of Gold Butte, Clark County, Nevada. Geol. Soc. Am. Bull. 73, 813–832.

Warnock, A.C., Zeitler, P.K., Wolf, R.A., Bergman, S.C., 1997. An evaluation of low-temperature apatite U–Th/He thermochronometry. Geochim. Cosmochim. Acta 61, 5371–5377.

Wasserburg, G.J., Lanphere, M.A., 1965. Age determinations in the Precambrian of Arizona and Nevada. Geol. Soc. Am. Bull. 76, 753–758.

Wernicke, B.P., Axen, G.J., 1988. On the role of isostasy in the evolution of normal fault systems. Geology 16, 848–851.

Wolf, R.A., Farley, K.A., Silver, L.T., 1996. Helium diffusion and low-temperature thermochronometry of apatite. Geochim. Cosmochim. Acta 60, 4231–4240.

Wolf, R.A., Farley, K.A., Silver, L.T., 1997. Assessment of (U–Th)/He thermochronometry: the low-temperature history of the San Jacinto mountains, California. Geology 25, 65–68.

Wolf, R.A., Farley, K.A., Kass, D.M., 1998. Modeling of the temperature sensitivity of the apatite (U–Th)/He thermochronometer. Chem. Geol. 148, 105–114.

Yamada, R., Tagami, T., Nishimura, S., Ito, H., 1995. Annealing kinetics of fission tracks in zircon: an experimental study. Chem. Geol. 122, 249–258.

Zeitler, P.K., Herczig, A.L., McDougall, I., Honda, M., 1987. U–Th–He dating of apatite: a potential thermochronometer. Geochim. Cosmochim. Acta 51, 2865–2868.